CHARACTERIZATION OF THIOL-DISULFIDE SYSTEMS AS CANDIDATES TO COMBAT OXIDATIVE STRESS

Ph.D. Thesis

Juliana Ferreira de Santana

The Doctoral School of Pharmaceutical Sciences

Semmelweis University

Supervisors: Béla Noszál, D.Sc.

Consultant: Arash Mirzahosseini, PharmD, Ph.D.

Official reviewers: Ádám Orosz, PharmD, Ph.D. and Fanni Sebák, PharmD, Ph.D.

Head of the Complex Examination Committee: Éva Szökő, D.Sc.

Members of the Complex Examination Committee: Zsolt Szakonyi, D.Sc. and Viola Tomási, Ph.D.

Budapest
2022

1. Introduction

1.1 Oxidative stress and redox signaling

The term “oxidative stress” was formulated by Helmut Sies in 1985. First, it was delineated as “a disturbance in the prooxidant-antioxidant balance in favor of the former”. In 2007, to incorporate the term redox signaling the definition was updated to “an imbalance between oxidants and antioxidants in favor of the oxidants, leading to a disruption of redox signaling control and/or molecular damage”. This imbalance in favor of oxidants has been associated with aging, atherosclerosis, carcinogenesis, diabetes, and neurodegeneration.

The oxidants usually referred to as reactive oxygen species (ROS), are produced chiefly within the mitochondria throughout the traditional cellular metabolism. However, within the cytosol and plasma membrane, some enzymes like NADPH oxidase and cytochrome P450 oxidase can originate them as well. ROS have a vital role against infectious agents and in cellular signaling systems. Although their effects are beneficial

only if they are present in low or moderate concentrations. In higher concentrations they can be toxic to organisms, nevertheless, through billions of evolution years, cells became capable to evolve antioxidant molecules and detoxifying enzymes to deal with them.

Reactive oxygen species comprise both free radicals and nonradical oxygen derivatives. Free radicals are chemical species with an unpaired electron, which are responsible for the high reactivity of these compounds. Some examples of free radicals include hydroxyl radical ($OH^{\bullet}$) and superoxide anion ($O_2^{\bullet -}$), while nonradical oxygen derivatives can also be chemically stable molecules, such as hydrogen peroxide (H_2O_2) and organic hydroperoxide (ROOH).

In previous researches, the centre of attention was mostly free radicals, which persist as a crucial topic. However, studies showed that hydroperoxides and electrophiles also have fundamental functions in physiologically signaling and regulation of transcription factors. Redox signaling is part of the physiology of cells.

It can be defined as a process in which the signal is transported through redox reactions and has a compelling role in pathophysiological responses. For redox signaling to occur, an unbalanced redox state is necessary by decreasing the activity of antioxidants or increasing ROS generation.

In the signaling pathways, it is important to figure out how ROS can modify a function of proteins. The two principal target residues in the redox regulation are the sulfur-containing cysteine (Cys) and methionine (Met) in proteins. Cys oxidation develops reactive sulfenic acid (–SOH) which can form disulfide bonds (– S – S –) with nearby Cys or go through further oxidation to sulfinic (–SO_2H) or sulfonic (–SO_3H) acid. These types of Cys oxidation are noticed when a protein has its activity modified and may become vulnerable to aggregation and/or degradation. It does not imply that Cys is the only amino acid in redox signaling, but those are the Cys chemical reactions that mainly determine redox signaling containing hydroperoxides and some other electrophiles.

To date there is not, unfortunately, any powerful therapeutic agent to treat chronic diseases generated by oxidative stress. It is currently an unmet medical need to have a therapy based on small molecules such as antioxidants to control oxidative stress.

2. Objectives

- The goal of our work is to see whether a correlation anticipated in previous work from our group, really exists between the redox potential, and the NMR chemical shifts of nuclei near the sulfur atom in these compounds.
- Determination of limiting ^{1}H and ^{13}C chemical shifts of 13 compounds (thiols and disulfides) and 15 Cys containing peptides.
- The hypothesized correlation is expected on the basis of changing electron densities, which are concomitant influencers of both the redox and NMR parameters.
- The correlations were analysed by plotting microscopic log*k* values pertaining to the thiolate group in various microspecies and the corresponding chemical shift values.

3. Results

3.1 Materials

All the thiols and disulfides studied were obtained from Sigma-Aldrich (Saint Louis, MO, USA) and used without further purification. Except for the compounds 4-methoxybenzoylcysteine amide, 4-nitrobenzoylcysteine amide, 4-dimethylaminobenzoylcysteine amide, 3,5-bis(trifluoromethyl)benzoylcysteine amide, all the peptides containing Cys, were purchased from ProteoGenix (Schiltigheim, France). Their homodisulfides were created by adding 1% H_2O_2 to the thiols. Deionized water was produced in our laboratory by a Milli-Q Direct 8 Millipore system.

The Cys derivative compounds 4-methoxybenzoylcysteine amide, 4-nitrobenzoylcysteine amide, 4-dimethylaminobenzoylcysteine amide, 3,5-bis(trifluoromethyl)benzoylcysteine amide were synthesized on TentaGel R RAM resin (0.19 mmol/g) with

Fmoc-chemistry on a Rink amide linker on a 0.1 mmol scale manually. The coupling of Cys was performed as follows: 3 equivalents of Fmoc-protected amino acid, 3 equivalents of the uronium coupling agent O-(7-azabenzotriazol-1-yl)-N, N, N′, N′-tetramethyluronium hexafluorophosphate (HATU) and 6 equivalents of N, N-diisopropylethylamine (DIPEA) were used in N, N-dimethylformamide (DMF) as solvent with shaking for 3 h. After the coupling steps, the resin was washed 3 times with DMF, once with methanol, and 3 times with dichloromethane. Deprotection was performed with 2% 1,8-diazabicyclo[5.4.0]undec-7-ene (DBU) and 2% piperidine in DMF in two steps, with reaction times of 5 and 15 min. After the deprotection of the Fmoc-group, the resin was washed and a further coupling step was carried out with the appropriate benzoic acid derivative and HATU with DIPEA as the coupling agent. The resin was washed with the same solvents as delineated previously. The cleavage was performed with trifluoroacetic acid/water/DL-dithiothreitol (DTT)/triisopropylsilane

(TIS) (90:5:2.5:2.5) at 0 °C for 2 h. The cleavage cocktail was evaporated, and the peptide was precipitated with diethyl ether. After the precipitation, the Cys derivatives were dissolved in a 10% acetic acid solution and were lyophilized. As a final purification, the solid residue that remained after lyophilization was digerated with diisopropyl ether. The crystals gained by this step were washed with diisopropyl ether.

3.2 NMR spectroscopy measurements

NMR spectra were recorded on a Varian 600 MHz spectrometer at 298.15 ± 0.1 K. The solvent was H_2O:D_2O 95:5 (V/V), and ionic strength was adjusted to 0.15 mol/L. The pH values were determined *in situ* by internal indicator molecules (at ca. 1 mmol/L) optimized for ^1H NMR. The sample volume was 550 μL and every sample contained ca. 1 mmol/L DSS (3-(trimethylsilyl)propane-1-sulfonate) as a chemical shift reference. The H_2O ^1H signal was suppressed with a presaturation sequence; the average acquisition parameters for ^1H measurements were: number of transients = 16, number of points =

65536, acquisition time = 3.33 s, relaxation delay = 1.5 s. ^{1}H-^{13}C HSQC measurements were performed with solvent signal presaturation and the following parameters: number of transients = 64, number of increments = 96, number of points = 2884, acquisition time = 149.968 ms, relaxation delay = 1 s.

3.3 Statistical Analysis

Non-linear regression analysis on the titrations were performed using R version 4.0.5 (R Foundation for Statistical Computing, Vienna, Austria) with the function on equation (1):

$$\delta_{\mathrm{obs}}(\mathrm{pH}) = \frac{\delta_{\mathrm{L}} + \delta_{\mathrm{HL}} \times 10^{\log K - \mathrm{pH}}}{1 + 10^{\log K - \mathrm{pH}}} \qquad (1)$$

where δ_{L} is the chemical shift of an unprotonated moiety, δ_{HL} is the chemical shift of the protonated moiety, and log$K$ is the base 10 logarithm of the group-specific protonation constant. Linear regression analyses for the chemical shift-log$K$ data were carried out using the R version 4.0.5 (R Foundation for Statistical Computing, Vienna, Austria).

4. Discussion

In this work, we analysed NMR spectra from Cys, CysSSCys, CysASH, CysASSCysA, Hcy, HcySSHcy, PenA, penicillamine-disulfide, and cysteine-containing peptides to determine their thiolate basicities and the related standard redox potential. The redox potential values were calculated from log*k* in previous works by Mirzahosseini and Noszál. Although Cys as amino acid or moiety is the main regulator of redox homeostasis and signaling, not all Cys residues are expected to be oxidized, it will rely on the solvent accessibility, thiolate basicity, and polarity of the nearby residues. Through the $^{13}C/^{1}H$ chemical shift analysis, a direct and inverse relationship could be identified between them and log*k*, respectively.

Due to the different chemical shift ranges, the ^{1}H protonation shifts are considerably lower compared to the ^{13}C counterparts. Besides that, there are smaller differences between the reduced and oxidized species in terms of ^{1}H chemical shifts as well. In contrast, the ^{13}C chemical shift data of the $^{\alpha}CH$ reveal the redox state of the

species and significant physicochemical properties. It is worthy to mention a strong linear relationship between almost every nucleus chemical shifts and thiolate basicities, but particularly in the $^{\alpha}$CH nuclei, in both ^{1}H and ^{13}C NMR. To support this finding, in a preceding work, Sharma and Rajarathnam already showed that α and β ^{13}C NMR chemical shifts can clearly indicate disulfide bond structure and recognize the reduced and oxidized state of Cys.

It was feasible to notice a better correlation between all chemical shift data and logK in compounds shown in Figure 1. As PenA has lower thiolate basicity, likely due to the shielding effect of the two methyl groups restrained near the thiolate, it is significant to observe that the correlation is maintained. Nevertheless, it is still essential to expand this model to compounds with even lower thiolate basicity.

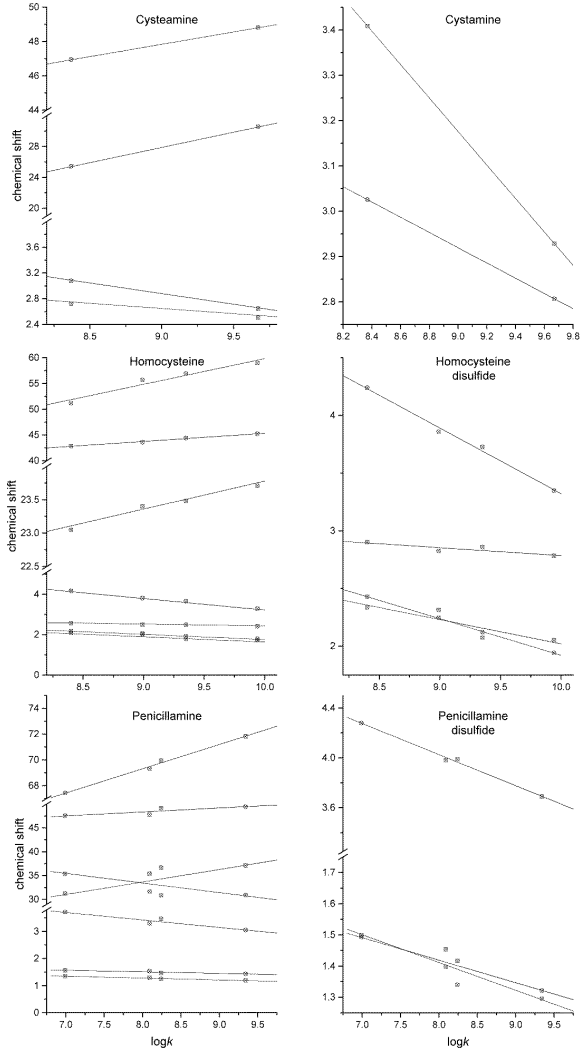

Figure 1. *The multivariate linear regression fits of the chemical shift data vs thiolate basicities.*

Regarding the protonation constant results of the cysteine-containing peptides from this work, it is newsworthy to observe that the neighboring residue on a Cys has virtually no bearing on the acid-base properties of the Cys thiolate, implying that the properties of a Cys side-chain can only be perturbed via steric interactions in a peptide. The regression analysis displayed in Figure 2 shows a linear relationship within the data of Cys and CysSSCys microspecies, whereas the correlation data from cysteine-containing peptides only show adherence for the case of $^{\alpha}CH$ ^{13}C. This nucleus reveals the best conformity to the correlation. Consequently, this is the best option to estimate thiolate properties from NMR data. This is probably because the $^{\alpha}CH$ carbon and the sulfur atom are connected via two covalent bonds. The $^{\alpha}CH$ ^{1}H chemical shifts of the Cys, however, are presumably perturbed more by the protonation state of adjacent moieties or the presence of a peptide bond, which makes this nucleus a poor indicator on the properties of the status of the sulfur atom. The $^{\beta}CH_2$ nuclei also demonstrate this

phenomenon and have a weaker correlation with log*K* altogether. These observations hold for the regression analysis of the thiolate bearing species as well as that of the thiol bearing and the corresponding disulfide bearing species.

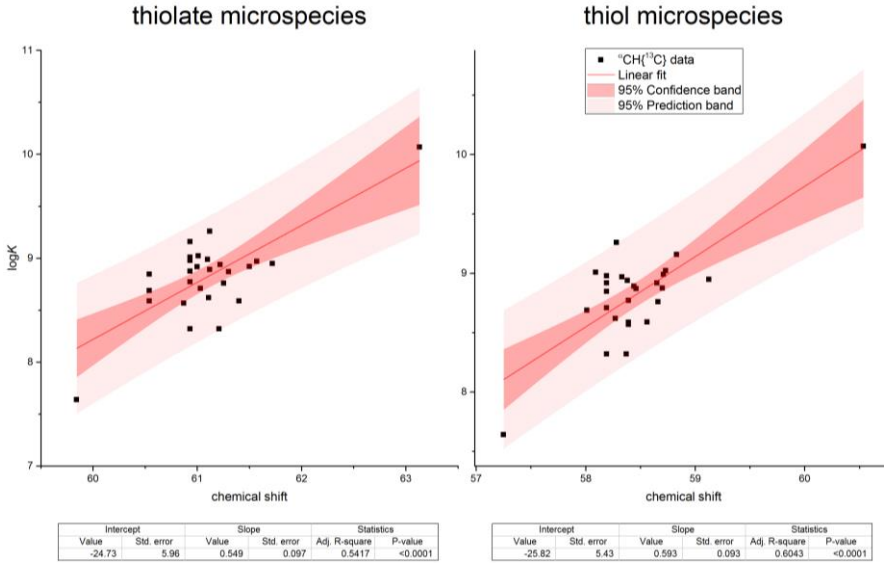

Intercept		Slope		Statistics	
Value	Std. error	Value	Std. error	Adj. R-square	P-value
-24.73	5.96	0.549	0.097	0.5417	<0.0001

Intercept		Slope		Statistics	
Value	Std. error	Value	Std. error	Adj. R-square	P-value
-25.82	5.43	0.593	0.093	0.6043	<0.0001

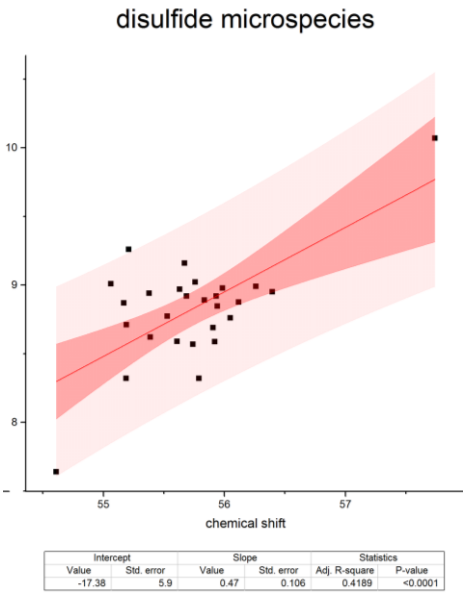

Figure 2. *The univariate linear regression fits of the $^{\alpha}CH$ ^{13}C data together with 95% confidence and prediction bands.*

It is frequently assumed that chemical shifts of the NMR active nuclei are highly susceptible to changes in the intramolecular microenvironment. Besides that, the correlation from cysteine-containing compound chemical shifts, log*K*, and redox potentials could bring better

knowledge about the chemistry and the biological function of its oxidation. Through the gathered chemical shift data set and regression analysis, it is also possible to estimate thiolate basicity/thiol acidity and the concomitant standard redox potential.

Even though, the clear limitation of this method is the window of the regression analysis. Whereas the species-specific thiolate basicities observed in the compounds analysed are limited to a certain range, and the further analysis of derivative compounds did not extend this range (the lowest value analysed was from PenA), in order to extend the scale of the regression more measurements on larger peptides are needed. A detailed literature search for reported thiolate log*K* values in the PKAD Database and the corresponding chemical shift values for the Cys residue using the Biological Magnetic Resonance Data Bank (BMRM) (http://www.bmrb.wisc.edu) was performed. Unfortunately, the literature review generated only a handful of data, that were not reliable enough to

incorporate into the model. Thereby our research group is currently investigating larger peptides as we hope that the determination of species-specific chemical shifts of added peptides will extend the regression model for better utility.

5. Bibliography of candidate's publications

1. **Santana, J. F.;** Mirzahosseini, A.; Noszál, B.. Correlation between the NMR chemical shifts and thiolate protonation constants of cysteamine, homocysteine, and penicillamine. Journal of Spectroscopy, 2022: 9491360-9491368, 2022 - https://doi.org/10.1155/2022/9491360
   Impact Factor: 1.750

2. **Santana, J.F.;** Mirzahosseini, A.; Mándity, B.; Bogdán, D.; Mándity, I. and Noszál, B.. Close correlation between thiolate basicity and certain NMR parameters in cysteine and cystine microspecies. PLoS ONE 17(3): e0264866, 2022 -

https://doi.org/10.1371/journal.pone.0264866.
Impact Factor: 3.752

5.1 Publications pertaining to different subjects

3. Soares, B.A.; Teixeira, K.N.; **de Santana, J.F.;** de Assis, B.L.M.; Zocatelli-Ribeiro, C.; Scandelari, J.P.S.; Thomaz-Soccol, V.; Machado-de-Ávila, R.A.; Alvarenga, L.M.; de Moura, J.. Epitope mapping from *Mycobacterium leprae* proteins: Convergent data from *in silico* and *in vitro* approaches for serodiagnosis of leprosy, Molecular Immunology, Vol. 138, 2021 - https://doi.org/10.1016/j.molimm.2021.07.021

4. **De Santana, J.F.;** da Silva, M.R.B.; Picheth, G.F.; Yamanaka, I.B.; Fogaça, R.L.; Thomaz-Soccol, V.; Machado-de-Avila, R.A.; Chávez-Olórtegui, C.; Sierakowski M.R.; de Freitas, R.A.; Alvarenga, L.M.; de Moura, J..Engineered biomarkers for leprosy diagnosis using labeled and label-free

analysis, Talanta, Vol. 187, 2018 - https://doi.org/10.1016/j.talanta.2018.05.027

5. **De Santana, J.F.;** Pilla, V.; Silva, A.C.; Dantas, N.O.; Messias, D.N.; Andrade, A.A.. Optical characterization of core-shell quantum dots embedded in synthetic saliva: Temporal dynamics, Journal of Photochemistry and Photobiology B: Biology, Vol. 151, 2015 - https://doi.org/10.1016/j.jphotobiol.2015.08.016

6. Pilla, V.; Alves, L.P.; **de Santana, J.F**; da Silva, L.G.; Ruggiero, R.; Munin, E.. Fluorescence quantum efficiency of CdSe/ZnS quantum dots embedded in biofluids: pH dependence, Journal of Applied Physics, Vol. 112, 2012 - https://doi.org/10.1063/1.4767470